Quantum Mechanical/Molecular Mechanical Study on the Favorskii Rearrangement in Aqueous Media

R. Castillo, J. Andrés, and V. Moliner*

Departament de Ciències Experimentals, Universitat Jaume I, Box 224, 12080 Castelló, Spain

Received: September 13, 2000; In Final Form: January 10, 2001

In this paper, hybrid quantum mechanical/molecular mechanical (QM/MM) calculations including 500 water molecules mold solvent effects on the molecular mechanisms of the α-chlorocyclobutanone and α-chlorocyclohexanone transpositions to yield cyclopropane and cyclopentane carboxylic acids, respectively, as a model of the Favorskii rearrangement. The two accepted molecular mechanisms, the semibenzilic acid and the cyclopropanone transpositions, as well as the competition between both reaction pathways and the ring size effects are addressed in this investigation. Stationary points—reactants, products, transition structures, and intermediary species along both reaction pathways—have been located and characterized, involving a fully flexible active-site region, by means of GRACE and CHARMM software. The transition structures have been connected with their respective reactants and products by the intrinsic reaction coordinate procedure carried out in the presence of water media, thus obtaining for the first time a realistic reaction pathway for this chemical transposition. The analysis of the results obtained by QM/MM methods shows that the semibenzilic acid mechanism is favored over the cyclopropanone mechanism for the α-chlorocyclobutanone system. However, the study of the ring size effects reveals that the cyclopropanone mechanism is the energetically preferred reactive channel for the α-chlorocyclohexanone ring, probably due to the straining effects on bicycle cyclopropanone, an intermediate that appears on the semibenzilic acid pathway. This later mechanism is described as a two-step one, while the cyclopropanone or Loftfield mechanism is for the first time described as a four-step reaction. These results provide new information on an important chemical reaction and the key factors responsible for the behavior of reactant systems embedded in aqueous media. This methodology allows evaluation of specific solute−solvent interactions as well as weighing up of the different energy contribution terms.

1. Introduction

In recent decades quantum mechanical calculations have been gradually recognized as a useful tool in research related to the elucidation of molecular reaction mechanisms.[1,2] The understanding at molecular level of a reaction mechanism for a given chemical reaction requires a detailed knowledge of stationary points: reactants, transition structure (TS), products, and possible intermediates on the potential energy surface (PES). In particular, the theoretical characterization of TSs provides a source of information, independent from experimental studies, concerning the geometry, electronic structure, and stereochemistry along the reaction pathway.[3] Environmental effects play a fundamental role in many chemical processes such as equilibria and reactions. The solvent can often influence the rate of conversion in a particular chemical reaction and can also affect the outcome of the reaction by favoring one particular reaction pathway when alternative paths are possible. It is, therefore, important to understand the interactions of the solvent with the reacting species on a molecular level to study chemical reactions in solution or in a protein medium.

The theoretical treatment of the solvent can be broadly classified in two categories: discrete models and continuum models. In the discrete models, solvent molecules are treated explicitly, allowing the description of both the microscopic structure of the solvent and the specific solute−solvent interaction. In practice, if the system is described by quantum mechanics, the applicability of the discrete models, a supermolecule approach, is restricted to a selected number of configurations of a solute sorrounded by a few solvent molecules.[4,5] However, it does not enable the characterization of long-range bulk solvent forces. Moreover, the number of solvent molecules required to properly represent the medium for a given solute would be so large that performing a quantum chemical calculation in such a system becomes prohibitively expensive. Conversely, statistical simulations using empirical interaction potentials allow calculations with a large number of both solvent molecules and configurations.[6−8] However, they cannot account for the changes induced by the solvent in the electronic structure of the solute and they cannot give a very accurate description of the electronic structure of the solute when chemical reactions are involved. On the other hand, the continuum models allow the incorporation of solvent effects but neglect the microscopic solvation structure in the vicinity of the solute.[9−12] A large number of such methods have been developed.[13,14] In these methods, the solute is embedded in a cavity while the solvent, treated as a continuous medium having the same dielectric constant as the bulk liquid, is incorporated in the solute Hamiltonian as a perturbation. In this reaction field approach, the bulk medium is polarized by the solute molecules and subsequently back-polarizes the solute, etc.

Much attention has been focused recently on alternative approaches based on hybrid methods,[15−22] combining quantum

* To whom correspondence should be addressed.

10.1021/jp003264g CCC: $20.00
Published on Web 03/06/2001

SCHEME 1

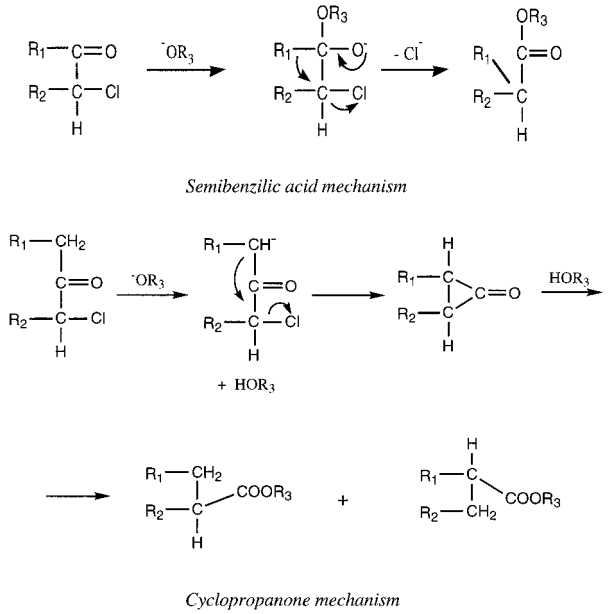

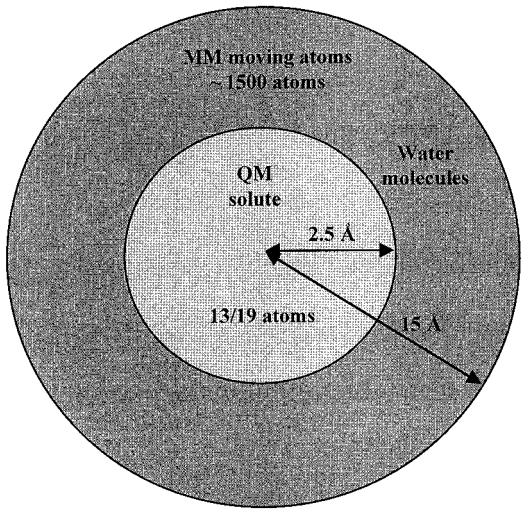

Figure 1. Schematic diagram of how the hybrid potential simulation system was partitioned into the different regions. The QM region contain 13 or 19 atoms for α-chlorocyclobutanone or α-chlorocyclohexanone, respectively, whereas the inner MM region, that contained atoms free to move, had 500 water molecules.

mechanics with classical force fields, which allows the proper treatment of the chemical processes but still retains computational efficiency. These methods include a classical simulation of the solvent terms and solute−solvent interactions coupled to a quantum mechanical description of the solute, providing valuable results.[23−30] These methods are based on the fact that the reacting system is usually limited to a small number of atoms, which undergoes most of the electronic changes associated with chemical reactivity and is described by a quantum mechanical (QM) method. The rest of the atoms, which do not require the making or the breaking of chemical bonds, are represented by a standard molecular mechanical (MM) force field. The resulting coupling QM/MM provides a suitable potential that can model the chemical reactivity of a wide range of complex systems in different fields such as solution chemistry,[31−34] enzyme catalysis,[26,29,30,35−40] transition metal complexes,[41−43] surface reactivity,[44−46] zeolites,[46,47] and crystal formation.[48]

Originally described in 1894,[49] Favorskii reaction corresponds to the nucleophilic attack of bases, e.g., hydroxide, alkoxide ions, or amines, on α-halo ketones to yield the salts, esters, or amides of the corresponding carboxylic acids, respectively, with a skeleton of the same number of carbon atoms.[49−55] Due to its versatility, it has become an increasingly reliable and specialized instrument of organic synthesis, and an appreciable number of experimental works on this rearrangement and its applications can be found in the recent literature.[56−65] Nevertheless, some controversy over the nature of the molecular mechanism of this reaction persists and at least five mechanisms have been proposed.[66−73] According to the current bibliography, only two of the proposed mechanisms have been supported by most of the evidence and remain as the accepted mechanisms: the Loftfield cyclopropanone mechanism[72,73] and the semibenzilic acid one,[70] depicted in Scheme 1.

The vast majority of chemical reactions are performed in solution and the need to increase knowledge about interactions between solvent and solute remains crucial. It is known that the reactivity of a chemical species depends on the solvent associated around the molecules. Our research program has long maintained an interest to the theoretical treatment of solvent effects in chemical reactivity studies.[74−77] In previous theoretical works,[27,77] the Favorskii reaction of α-chlorocyclobutanone has been studied with ab initio and semiempirical methods. In these papers, the electrostatic interactions with the bulk solvent were introduced by means of the continuum model of Rivail and Rinardi,[78] with the SCRFPAC package[79] added to the GAUSSIAN92 program[80] at the HF/6-31G* level,[27] and with the conductorlike screening model (COSMO)[81] proposed by Klamt and Schüürmann implemented in the MOPAC[82] for the PM3 semiempirical calculations.[77] In this later study, two discrete water molecules were also introduced in the molecular model. Therefore it seems of interest to extend these studies by using hybrid quantum mechanical and classical potentials methods in order to increase the understanding of the molecular events by which solvent (water) interacts with the reacting system along the two most accepted reaction pathways of the Favorskii rearrangement. Furthermore, two solutes, α-chlorocyclobutanone and α-chlorocyclohexanone, have been employed in order to analyze the solute ring size effect. In this work, we present accurate results with a view to understanding the importance of the solvent in these reaction mechanisms, including a comparison with our previous mentioned studies.[27,77]

2. Model Systems and Computing Procedure

We used two different molecular models, α-chlorocyclobutanone (B) and α-chlorocyclohexanone (H) reacting systems, whose initial structures have been derived from previous optimized geometries obtained in gas phase. The system was hydrated within a 15 Å radius TIP3P[83] water molecules sphere centered on the carbon atoms of the corresponding rings (overlapping water molecules were deleted). Finally, a solvent boundary potential[84] was applied to the water molecules in order to maintain the structure of the water at the edges of the system. Then, the system was divided into QM and MM regions: the α-chlorocyclobutanone and α-chlorocyclohexanone rings and the hydroxyl anion were included into the QM zone, while the water molecules were treated classically. The resulting molecular system was a pseudosphere of a total amount of ca. 1500 atoms. A schematic diagram of how the hybrid potential simulation system was partitioned into different regions is depicted in Figure 1.

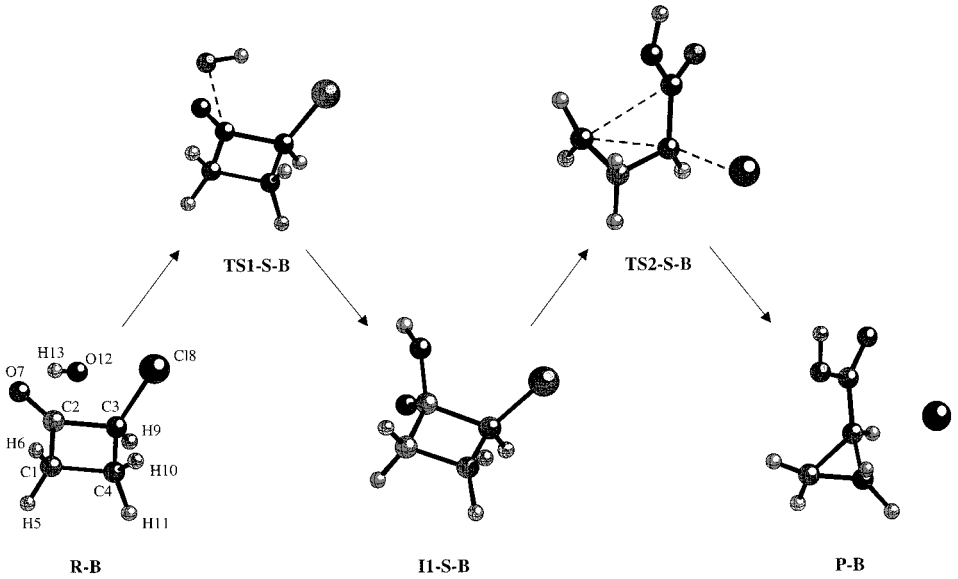

Figure 2. Representation of the stationary point structures of the solute for the semibenzilic acid mechanism for model B.

Once the system was prepared, the hybrid QM/MM optimizations were carried out, where the QM atoms of the reacting system were treated by the AM1 semiempirical molecular orbital method and the MM atoms were minimized by means of the ABNR algorithm. The CHARMM24 program[85] was used for all the QM/MM optimizations.

As explained in the previous sections, the theoretical description of the main chemical processes that take place in a reaction requires the complete characterization of the stationary points on the PES. To make this representation available, we have proceeded to investigate grids for every step of the reaction, defined by internal coordinates that were fixed at each point, and all other degrees of freedom, for each respective point, were submitted for QM/MM optimization by means of the CHARMM24 program.

GRACE,[26,35,86] combined with CHARMM, has allowed the QM/MM search of TSs, saddle points of index one, by use of an eigenvector-followed (EF) algorithm. A partial rational function operator/adopted-basis Newton−Raphson method is employed, utilizing a Hessian matrix describing the curvature of the QM/MM energy hypersurface for a subset of the system (containing all the quantum atoms of the model), together with a diagonal Hessian with the rest of the system updated. The root-mean-square (rms) residual gradient for all the molecular system is less than 0.005 kcal mol^{-1} $Å^{-1}$ in the optimized structures; this residual gradient is lower than the commonly accepted convergence criteria for optimized geometries of small molecules in quantum chemistry. This technique has been successfully carried out starting with a molecular structure selected from the quadratic regions of the PESs obtained with CHARMM. Once the structure was fully optimized, GRACE was used to trace the intrinsic reaction coordinate (IRC) path from the putative TS in each direction, leading to reactantlike and productlike structures, to demonstrate conclusively that the reported structure was indeed the TS for the correct step. Finally, the TS structure was characterized by determination of the vibrational frequencies. It is important to point out that the structures presented in this paper do not have to be considered as unique; as pointed out by Truhlar for reactions in solution[14] and by ourselves for reactions in enzymes,[35] many nearly degenerate stationary point structures can be located with very similar solute/substrate properties differing mainly in the conformation of the environment molecules. Nevertheless, considering the flexible character of our QM/MM model, the solute structures that emerge from the calculations can be used to discriminate between alternative mechanisms and to understand the role of the solvent.

3. Results and Discussion

It is important to realize that in the study of a chemical reaction the finding of one TS does not exclude the possibility of alternative reaction paths having other TSs. To discriminate between alternative molecular mechanisms for the Favorskii rearrangement, an extensive exploration of the PESs has been carried out. The solute structures associated with the stationary points along both reaction pathways (semibenzilic acid and cyclopropanone mechanisms) are illustrated in Figures 2 and 3 for the B model and in Figures 4 and 5 for the H model. The calculated structures are named as follows: the reactants, α-chlorocyclobutanone plus OH^- or α-chlorocyclohexanone plus OH^-, are designed by R-B and R-H, respectively, and the products cyclopropanecarboxylic acid plus Cl^- or cyclopentanecarboxylic acid plus Cl^- are named P-B and P-H, respectively. The structures corresponding to transition structures and intermediates are designated by the letters TS and I, respectively. The stationary points are distinguished from each other by appending the numbers 1, 2, etc., as they are introduced, and they are labeled with S or C for the semibenzilic acid mechanism or the cyclopropanone mechanism, respectively.

Some relevant interatomic distances of reactants, TS, intermediates, and products obtained for both mechanisms for both B and H systems are listed in Tables 1 and 2, while relative total energies of corresponding QM/MM optimized structures are given in Table 3. For sake of completeness the shapes of the corresponding reaction profiles are depicted in Figure 6.

The semibenzilic acid mechanism is presented as a two-step process (see Figures 2, 4, and 6a). The first step is a nucleophilic attack of OH^- on the C2 atom of the ring with formation of the corresponding intermediate. The second stage seems to be the rate-limiting step, via TS2-S-B or TS2-S-H, corresponding with the forming of the cyclocarboxylic acid with concomitant ring contraction and the C3−Cl•8 bond cleavage. This energetic profile obtained by means of QM/MM methods is quite similar to those obtained with the continuum models but only when the ab initio Hamiltonian was used,[27] since the semiempirical

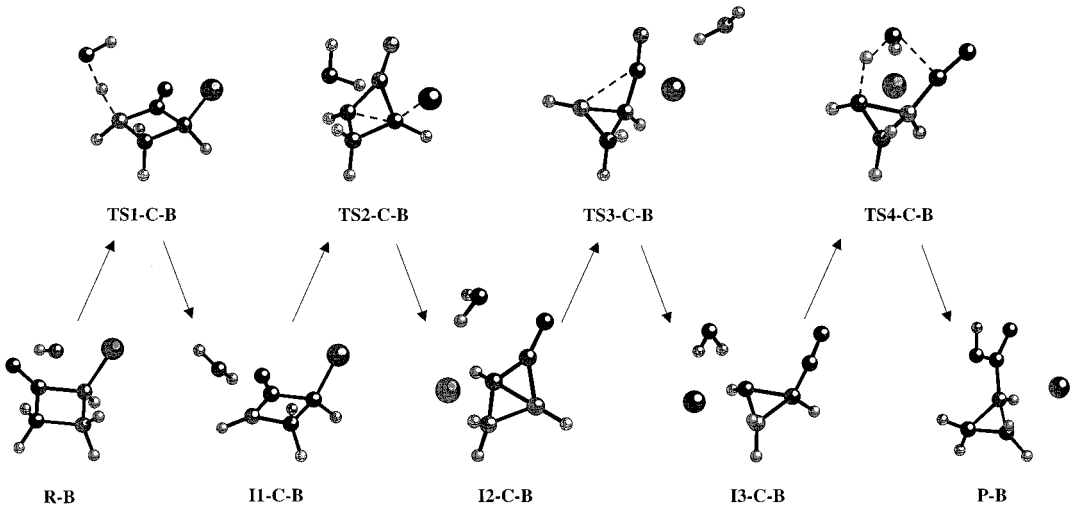

Figure 3. Representation of the stationary point structures of the solute for the cyclopropanone mechanism for model B.

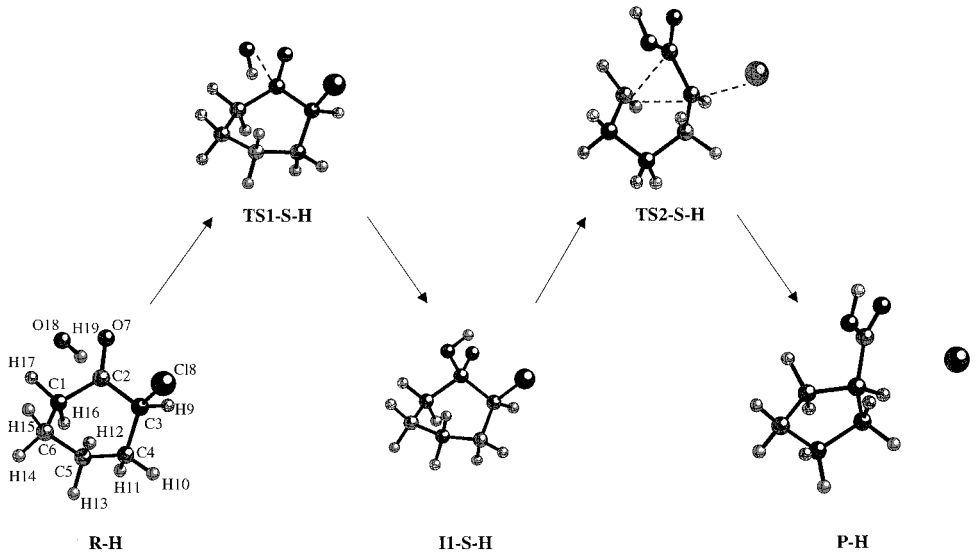

Figure 4. Representation of the stationary point structures of the solute for the semibenzilic acid mechanism for model H.

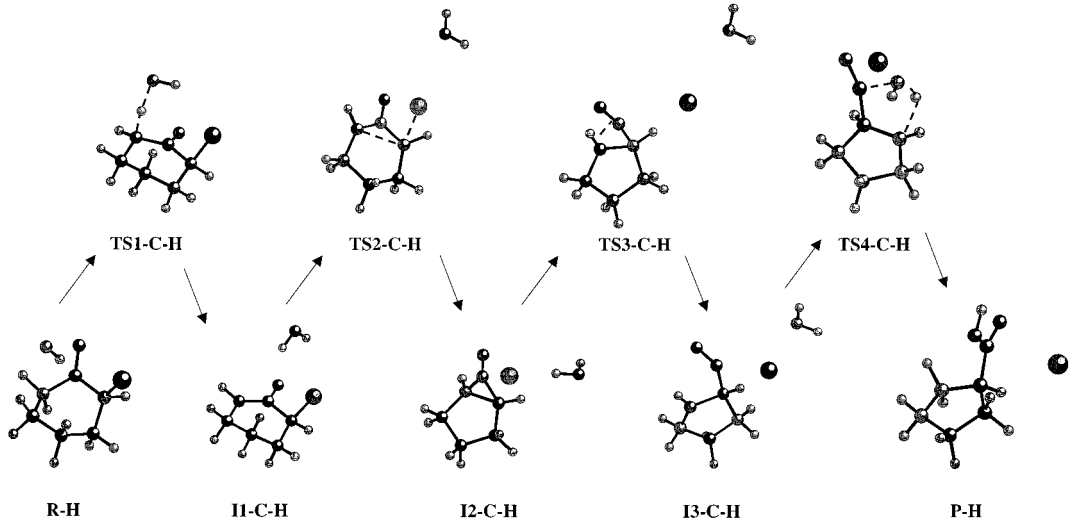

Figure 5. Representation of the stationary point structures of the solute for the cyclopropanone mechanism for model H.

one described the addition of the alkoxide to carbonyl carbon step in a barrierless fashion.[77] These previous energy profiles are also depicted in Figure 6 in order to appreciate the comparison. The intermediate region of the QM/MM PES is stabilized, thus increasing the barrier height of the second step. However, the geometrical results of the common stationary point structures render similar values for the bonds that are being formed and made along the transposition of B and H systems.

TABLE 1: Selected Geometrical Parameters of the Stationary Points for the B Model

	R-B	TS1-S-B	I-S-B	TS2-S-B	TS1-C-B	I1-C-B	TS2-C-B	I2-C-B	TS3-C-B	I3-C-B	TS4-C-B	P-B
C1−C2	1.516	1.520	1.564	2.404	1.477	1.384	1.436	1.461	2.091	2.387	2.449	2.555
C1−C3	2.194	2.193	2190	2.005	2.173	2.111	1.700	1.560	1.467	1.525	1.529	1.511
C2−O6	1.222	1.224	1.316	1.263	1.232	1.268	1.237	1.220	1.180	1.167	1.170	1.251
C3−Cl·8	1.731	1.730	1.748	2.103	1.737	1.754	2.586	4.264	3.912	4.654	4.297	3.676
C2−O12	3.301	2.401	1.418	1.364	3.354	4.000	3.698	3.187	3.455	3.422	2.126	1.349
C1−H11	1.120	1.111	1.108	1.088	1.285	2.220	3.633	4.110	4.641	1.720	1.505	1.105
H11−O12	2.257	2.391	2.523	2.512	1.347	0.968	0.973	0.961	0.981	1.006	1.125	3.968

TABLE 2: Selected Geometrical Parameters of the Stationary Points for the H Model

	R-H	TS1-S-H	I-S-H	TS2-S-H	TS1-C-H	I1-C-H	TS2-C-H	I2-C-H	TS3-C-H	I3-C-H	TS4-C-H	P-H
C1−C2	1.495	1.499	1.543	2.124	1.447	1.363	1.427	1.465	2.028	2.421	2.481	2.484
C1−C3	2.549	2.545	2.508	2.200	2.554	2.486	2.145	1.548	1.451	1.558	1.422	1.531
C2−O7	1.242	1.250	1.336	1.273	1.259	1.306	1.254	1.218	1.194	1.203	1.192	1.242
C3−Cl·8	1.763	1.761	1.776	2.208	1.775	1.790	2.972	3.265	3.164	3.198	3.376	3.273
C2−O18	3.315	2.303	1.441	1.379	3.133	3.381	7.567	6.056	3.712	3.854	1.749	1.359
C1−H17	1.122	1.122	1.119	1.103	1.274	3.064	8.226	4.562	4.105	4.218	2.065	1.119
H17−O18	3.682	2.866	2.656	2.699	1.430	0.967	0.965	0.981	0.967	0.968	0.997	3.026

TABLE 3: Relative Energies to Reactants of the Stationary Point Structures Located on the QM/MM PES[a]

	ΔE	ΔE_{QM}	ΔE_{int}	ΔE_{MM}	ΔE_{B3LYP}
R-B	0.0	0.0	0.0	0.0	0.0
TS1-S-B	3.33	−3.19	6.41	0.11	−13.67
I-S-B	−34.91	−59.17	28.09	−3.83	−72.82
TS2-S-B	38.28	−29.39	53.49	14.18	−75.31
TS1-C-B	5.23	−20.42	37.95	−12.28	−57.44
I1-C-B	−26.26	−44.56	50.78	−32.48	−65.28
TS2-C-B	27.37	2.26	37.05	−11.94	−45.01
I2-C-B	22.13	0.63	30.47	−8.97	−40.89
TS3-C-B	67.27	27.41	31.11	8.75	0.06
I3-C-B	60.37	39.2	4.93	16.25	4.39
TS4-C-B	64.91	32.38	18.62	13.91	−31.38
P-B	−40.18	−62.89	−4.49	27.2	−113.0
R-H	0.0	0.0	0.0	0.0	0.0
TS1-S-H	7.40	−1.49	8.28	0.61	−11.03
I-S-H	−28.86	−74.07	69.14	−23.93	−129.52
TS2-S-H	25.94	−19.76	70.76	−25.05	−66.23
TS1-C-H	8.55	−16.02	32.16	−7.59	−47.67
I1-C-H	−24.52	−56.33	56.04	−24.23	−65.70
TS2-C-H	15.76	11.44	−0.89	5.68	−3.00
I2-C-H	−8.30	−23.89	12.09	3.52	−63.55
TS3-C-H	31.75	20.66	10.43	0.65	−8.43
I3-C-H	28.68	−22.84	49.31	2.21	−66.56
TS4-C-H	34.19	7.11	49.30	−22.23	−22.53
P-H	−53.38	−50.70	9.28	−11.97	−64.62

[a] ΔE = total QM/MM barrier energy; ΔE_{QM} = in vacuo quantum single point energy using the solute structures optimized in the QM/MM calculations; ΔE_{int} = solvent−solute interaction energy; ΔE_{MM} = solvent−solvent interaction energy. All values are given in kilocalories per mole. ΔE_{B3LYP} = in vacuo B3LYP/6-31G* single point energy using the solute structures optimized in the QM/MM calculations.

This invariance is also supported by the comparable values of the net atomic charges on the solute molecules for the stationary points.

At this point in the discussion, we must point out that the optimized QM/MM structures labeled as R and P have been compared with the reactant complex and product complex that appear in our previous studies.[27,77] The methodology employed in the present work does not permit the realization of "real" reactant and product, as the solute is confined in a 15 Å sphere and we cannot put the species at an infinite distance one from each other. Nevertheless, we have obtained minimum energy structures for reactantlike and productlike structures with the OH^- and Cl^- at ca. 11 Å distance from the ring, respectively. These stationary point structures are12.73, 30.63, 3.91, and 0.50 kcal mol^{-1} lower in energy than R-B, P-B, R-H, and P-H, respectively. This stabilization is due to favorable hydrogen-bond interactions between the solute and the solvent water molecules.

The reaction pathway corresponding to the cyclopropanone mechanism for both B and H systems comprises four steps along three intermediates (see Figures 3, 5 and 6b). The first step is a base attack by hydroxide ion to give the deprotonated ciclopropanone ring. The second step corresponds with a cleavage of C3−Cl·8 bond and formation of a bicyclo intermediate. This step can be considered as an intramolecular nucleophilic substitution. The third step is an (unusual) heterolysis of a carbon−carbon bond (C1−C2), and finally the fourth step is an intramolecular general base-catalyzed hydration of the acylium moiety. An analysis of the results shows that TS3-C-B/TS3-C-H and TS4-C-B/TS4-C-H have the largest relative energetic values. A comparison of the imaginary frequency values shows that TS2-C-H and TS4-C-H present lower values than those corresponding with TS2-C-B and TS4-C-B. Furthermore, the reactive PES is flatter for the H system than the corresponding regions on the PES of the B system. An analysis and comparison of the geometrical data, in particular C3−Cl·8 (2.586 and 2.972 Å for TS2-C-B and TS2-C-H, respectively) C1−H11 (1.505 Å for TS4-C-B**)**, C1−H17 (2.065 Å for TS4-C-H), C2−O12 (2.126 Å for TS4-C-B), and C2−O18 (1.749 Å for TS4-C-H), show that the corresponding TSs of the second and fourth steps for the cyclopropanone mechanism are more dissociative at the H system than at the B one. These data are in accordance with the energetic and the commented topological results. These QM/MM results appear to differ from both previous mentioned solvent effect studies that described the Loftfield mechanism in three steps, although for different reasons. While in the combination of a semiempirical Hamiltonian and continuum dielectric medium results there is not any transition structure corresponding to the first step, the ab initio description of the solute in the presence of a continuum renders a profile where the hydration step of the bicyclo[1.1.0]-2-butanone intermediate takes place with concomitant ring contraction and formation of the products. A graphical comparison of all the energetic profiles is depicted in Figure 6b. From a thermodynamic point of view, the Favorskii rearrangements for B and H systems are described as very exothermic processes with relative values of the total energies of −40.18 and −53.38 kcal/mol, respectively.

The hybrid QM/MM calculations allow us to analyze the specific solute−solvent interactions as well as the different energy terms that contribute to the total energy. Thus, the total

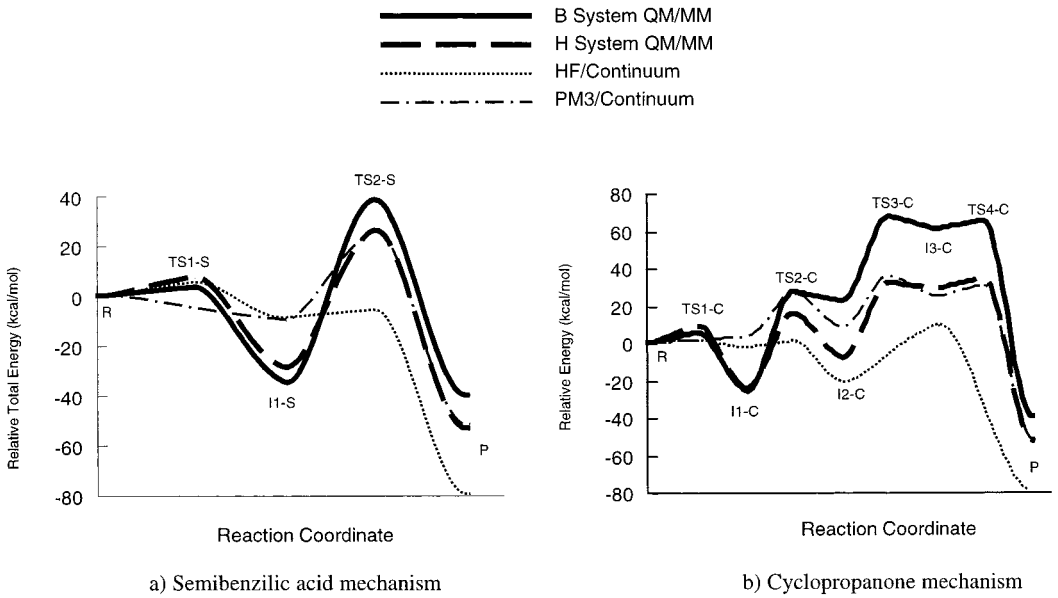

Figure 6. Schematic potential energy diagrams showing the total relative energies (kilocalories per mole) of the stationary points located on the reactive QM/MM PES. (a) Semibenzilic acid mechanism. (b) Cyclopropanone mechanism. Continuous lines correspond to α-chlorocyclobutanone system, while broken lines represent α-chlorocyclohexanone system. Dotted lines (···) represent the results of continuum models with an HF ab initio Hamiltonian (ref 27), while dotted−dashed lines (− · −) represent the profiles obtained with continuum models and a PM3 semiempirical description of the solute (ref 77).

QM/MM energies obtained in aqueous solution can be written as the following sum:

$$\Delta E = \Delta E_{QM} + \Delta E_{int} + \Delta E_{MM}$$

where ΔE_{QM} is the in vacuo AM1 single point energy calculation relative to R from the solute structures obtained in the QM/MM calculations, ΔE_{int} is the solvent−solute interaction energy relative to R, and ΔE_{MM} is the MM energy relative to R. The study of these energetic data (listed in Table 3), together with an analysis of the specific hydrogen bonds that appears between the different stationary point structures on the PES and water molecules of the first solvating shell, can be used as a guide to rationalize the solvent effects. Most of these interactions are done with the hydroxyl anion, the carbonyl group, and the chlorine anion, i.e., the charged moieties that are present at some stage of the reaction profile.

The results show the following trends:

(i) Although the solvent reorganization energy term, ΔE_{MM}, can be significant at some stationary point structures, the most important contributions to the relative total energies cames from the quantum energy (see ΔE_{QM} column of Table 3) and the solute−solvent interaction (see ΔE_{int} column of Table 3). (ii) For the B system, the large QM/MM interaction energy term presented in products ($\Delta E_{int} = -4.49$ kcal mol^{-1}) is associated with an increasing number of solute−solvent hydrogen-bond interactions when going from reactants to products. This trend is not observed in the H system, where the number of solute−solvent hydrogen bonds in reactants and products is almost invariant and ΔE_{int} is equal to 9.28 kcal mol^{-1}. (iii) For semibenzilic mechanism, the B solute system forms six hydrogen bonds with water molecules in all stationary point structures, except P-B, which presents nine. A hydration shell of four water molecules is found around the hydroxyl anion at R-B and TS1-S-B, four water molecules are hydrogen-bonded to the carbonyl group at I1-S-B and TS2-S-B, and a coordination sphere of six water molecules around the chlorine anion in found on P-B. Similar behavior is found for the H system; i.e., the charged moieties of the solute are forming interactions with the water molecules of the solvent. (iv) Nevertheless, a more accurate insight into these hydrogen bonds shows that, for instance, the four water−hydroxyl anion interaction distances are slightly longer in the TS1-S-B or TS1-C-B than in reactants, R-B, by ca. 0.1 Å. This fact could explain the origin of the first step barrier. The same trend is observed, for instance, in the second step, where the carbonyl group−water distances suffer an increment from the intermediate to the saddle point. (v) For cyclopropanone mechanism, the B system presents almost the same number of water molecules forming the first solvatation shell along the full reaction pathway as along the semibenzilic mechanism path. However, in the case of the H system, this number increases basically due to the fact that the hydroxyl anion is more accessible in the six-membered ring than in the four-membered one (O18 and the H19 atoms in the H system and O12 and H13 atoms in the B system).

Finally, it is important not to forget that a semiempirical Hamiltonian has been used to describe the quantum region in all QM/MM calculations. As a qualitative attempt to correct this possible source of error, we have calculated the single point energy of the AM1/TIP3P optimized substrates' structures using a more accurate method. The values obtained with the B3LYP[87] density functional method using the standard 6-31G* basis set are listed in the last column (ΔE_{B3LYP}) of Table 3. As expected, these energetic data in the ΔE_{B3LYP} column follows the same trend as the previous ΔE_{QM} column values but describe a profile much more stabilized. Thus, we could predict that future works based on ab initio/MM calculations will render smaller barriers on the reaction molecular mechanism.

4. Conclusions

In this work an attempt to characterize the molecular mechanisms of the Favorskii rearrangement of the α-chlorocyclobutanone and α-chlorocyclohexanone systems has been carried out. The method is based on the localization and characterization of stationary point structures (reactants, intermermediates, transition structures, and products) along two reaction profiles, semibenzilic acid and cyclopropanone path-

ways, on the potential energy surface by means of QM/MM methods. The use of the AM1 semiempirical Hamiltonian to describe the solute (the QM region) in which the reaction process takes place can be a source of criticism to our theoretical approach, so we must bear in mind that specific details of the process may change at higher levels of theory as, to some extent, demonstrated in the previous section (e.g., QM part treated by ab initio or density functional methods, inclusion of correlation energy, etc). Anyway, despite the approximate procedure of the calculations employed here, some important features were clarified. The present results show for the first time the nature of the molecular mechanism for the α-chlorocyclobutanone and α-chlorocyclohexanone transpositions, to yield the respective cyclocarboxylic acids, from QM/MM theoretical calculations.

The following conclusions can be drawn from the results reported in this study:

(a) The reaction along the semibenzilic acid mechanism for α-clorocyclobutanone and α-chlorocyclohexanone systems take place through a two-step mechanism. The first step is a nucleophilic attack of OH^- on the C2 atom of the ring with formation of the corresponding intermediate, while the second and rate-limting step is associated with the C1−C2 bond-breaking and C1−C3 bond-making processes. A comparison with the energy profile obtained previously from the continuum model for α-clorocyclobutanone shows that QM/MM methods increase the barrier heigth of the second step and the depth of the intermediate region.

(b) The Loftfield cyclopropanone mechanism seems to be a more complicated one. These new results reveal the existence of four transition structures instead of three that are usually presented in textbooks. The ab initio energy profiles obtained in the presence of a continuum dielectric model for α-clorocyclobutanone[27] did not describe the I3-C-B intermediate as a minimum on the PES, while if a semiempirical Hamiltonian was used to describe the solute in a cavity of a continuum medium[77] the transition structure associated with the H6 proton abstraction (i.e., the first R to I1 step) was not located.

(c) From energetics arguments, the comparison of these results with our previous calculations reveals that while the first model allowed us the use of ab initio level of calculation in a very easy way, the QM/MM model better reproduces specific solute−water molecule interactions and allows the use of larger molecular models. The former gives a more accurate description of the TS structure wavefunction of the solute, thus giving smaller barrier heights, but the latter permits us to analyze the effect of discrete hydrogen-bond interactions between the solute and the first solvation shell, as well as the overall solute−solvent energy interaction term.

(d) This study has also allowed us to weigh up the ring size effects. The comparison of both mechanisms obtained by means of the four- and six-membered rings, as molecular models of the solute molecule, reveal that smaller rings prefer the semibenzilic mechanism, while the energetically favored profile for bigger α-halo ketone rings seems to be the cyclopropanone mechanism. This result is in accordance with experimental studies reported in the literature by Chenier 20 years ago.[55]

Finally, the methodology presented here can be applicable to a wide variety of chemical reactions in solution, but we must note that equilibrium solvent effects have been computed. Thus, although the present results are very encouraging, a rigorous study should require ab initio/MM treatments and the dynamics of the whole system to study the myriad conformers that are present in solute−solvent systems.

Acknowledgment. This work was supported by research funds of the Ministerio de Educación, DGICYT (Project BQU2000-1425) and of the Foundation Caixa Castelló−Universitat Jaume I (Project 0I023.01/1). We are most indebted to Servei d'Informàtica de la Universitat Jaume I for providing us with multiple computing facilities. R.C. is grateful to BP Oil for a research fellowship.

References and Notes

(1) Skancke, P. N. *Acta Chem. Scand.* **1993**, *47*, 629.
(2) Williams, I. H. *Chem. Soc. Rev.* **1993**, 277.
(3) Stewart, J. D.; Liotta, L. J.; Benkovic, S. J. *Acc. Chem. Res.* **1993**, *26*, 396.
(4) Tapia, O.; Colonna, F.; Angyan, J. G. *J. Chem. Phys.* **1990**, *87*, 875.
(5) Castillo, R.; Moliner, V.; Andrés, J.; Oliva, M.; Safont, V. S.; Bohm, S. *J. Phys. Org. Chem.* **1998**, *11*, 670.
(6) Chandrasekhar, J.; Smith, S. F.; Jorgensen, W. L. *J. Am. Chem. Soc.* **1985**, *107*, 154.
(7) Allen, M. P.; Tildesley, D. J. *Computer Simulations of Liquids*; Clarendon Press: Oxford, 1987.
(8) McCammon, J. A.; Harvey, S. C. *Dynamics of Proteins and Nucleic Acids*; Cambridge University Press: Cambridge, U.K., 1987.
(9) Onsager, L. *J. Am. Chem. Soc.* **1936**, *58*, 1486.
(10) Rivail, J. L.; Rinaldi, D. *Chem. Phys.* **1976**, *18*, 233.
(11) Miertus, S.; Scrocco, E.; Tomasi, J. *J. Chem. Phys.* **1981**, *55*, 117.
(12) Cramer, C. J.; Truhlar, D. G. *Science* **1992**, *256*, 213.
(13) Cramer, C. J.; Truhlar, D. G. In *Solvent Effects and Chemical Reactivity*; Tapia, O., Bertrán, J., Eds.; Kluwer Academic Press: Dordrecht, The Netherlands, 1996; pp 1−80.
(14) Cramer, C. J.; Truhlar, D. G. *Chem. Rev.* **1999**, *99*, 2161.
(15) Warshel, A.; Levitt, M. *J. Mol. Biol.* **1976**, *103*, 227.
(16) Tapia, O.; Lamborelle, C.; Johannin, G. *Chem. Phys. Lett.* **1980**, *72*, 334.
(17) Singh, U. C.; Kollman, P. A. *J. Comput. Chem.* **1986**, *7*, 718.
(18) Bash, P. A.; Field, M. J.; Karplus, M. *J. Am. Chem. Soc.* **1987**, *109*, 8092.
(19) Bakowies, D.; Thiel, W. *J. Phys. Chem.* **1996**, *100*, 10580.
(20) Gao, J. *Acc. Chem. Res.* **1996**, *29*, 298.
(21) Matsubara, T.; Sieber, S.; Morokuma, K. *Int. J. Quantum Chem.* **1996**, *60*, 1101.
(22) Monard, G.; Loös, M.; Thery, V.; Baka, K.; Rivail, J. L. *Int. J. Quantum Chem.* **1996**, *58*, 153.
(23) Field, M. J.; Basch, P. A.; Karplus, M. *J. Comput. Chem.* **1990**, *11*, 700.
(24) Gao, J. *J. Am. Chem. Soc.* **1994**, *116*, 1563.
(25) Stanton, R. V.; Little, L. R.; Merz, K. M. *J. Phys. Chem.* **1995**, *99*, 483.
(26) Moliner, V.; Turner, A. J.; Williams, I. H. J. *Chem. Commun.* **1997**, 1271.
(27) Moliner, V.; Castillo, R.; Safont, V. S.; Oliva, M.; Bohm, S.; Tuñón, I.; Andrés, J. *J. Am. Chem. Soc.* **1997**, *119*, 1941.
(28) Monard, G.; Merz, K. M. J. *Acc. Chem. Res.* **1999**, *32*, 904.
(29) Moliner, V.; Andrés, J.; Oliva, M.; Safont, V. S.; Tapia, O. *Theor. Chem. Acc.* **1999**, *101*, 228.
(30) Andrés, J.; Oliva, M.; Safont, V. S.; Moliner, V.; Tapia, O. *Theor. Chem. Acc.* **1999**, *101*, 234.
(31) Cummins, P. L.; Gready, J. E. *J. Comput. Chem.* **1997**, *18*, 1496.
(32) Gao, J.; Li, N.; Freindorf, M. *J. Am. Chem. Soc.* **1996**, *118*, 4912.
(33) Gao, J.; Freindorf, M. *J. Phys. Chem. A* **1997**, *101*, 3182.
(34) Kaminski, G. A.; Jorgensen, W. L. *J. Phys. Chem. B* **1998**, *102*, 1787.
(35) Turner, A. J.; Moliner, V.; Williams, I. H. *Phys. Chem. Chem. Phys.* **1999**, *1*, 1323.
(36) Bentzien, J.; Muller, R. P.; Florian, J.; Warshel, A. *J. Phys. Chem. B* **1998**, *102*, 2293.
(37) Cummins, P. L.; Gready, J. E. *J. Comput. Chem.* **1998**, *19*, 977.
(38) Mulholland, A. J.; Richards, W. G. *Proteins: Struct., Funct., Genet.* **1997**, *27*, 9.
(39) Ranganathan, S.; Gready, J. E. *J. Phys. Chem. B* **1997**, *101*, 5614.
(40) Thomas, A.; Jourand, D.; Bret, C.; Amara, P.; Field, M. J. *J. Am. Chem. Soc.* **1999**, *121*, 9693.
(41) Matsubara, T.; Maseras, F.; Koga, N.; Morokuma, K. *J. Phys. Chem.* **1996**, *100*, 2573.
(42) Ujaque, G.; Cooper, A. C.; Maseras, F.; Eisenstein, O.; Caulton, G. A. *J. Am. Chem. Soc.* **1996**, *118*, 361.
(43) Maseras, F.; Lledos, A.; Duran, M. *J. Chem. Soc., Faraday Trans.* **1992**, *88*, 1111.
(44) Carmer, C. S.; Weiner, B.; Frenklach, J. *J. Chem. Phys.* **1993**, *99*, 1356.

(45) Gorb, L. G.; Rivail, J. L.; Thery, V.; Rinaldi, D. *Int. J. Quantum Chem.* **1996**, *60*, 313.
(46) Lopez, N.; Pacchioni, G.; Maseras, F.; Illas, F. *Chem. Phys. Lett.* **1998**, *294*, 611.
(47) Sherwood, P.; de Vries, A.; Collins, S. J.; Greatbanks, S. P.; Burton, N. A.; Vicent, M. A.; Hillier, I. H. *Faraday Discuss.* **1997**, *106*, 79.
(48) Ferenczy, G. G.; Csonka, G. I.; Náray-Szabó, G. I.; Ángyán, J. G. *J. Comput. Chem.* **1998**, *19*, 38.
(49) Favorskii, A. E. *J. Russ. Phys. Chem. Soc.* **1894**, *26*, 559.
(50) Kende, A. S. *Organic Reactions*; Wiley: New York, 1960; Vol. 11, p 261.
(51) Akhrem, A. A.; Ustynynk, T. K.; Titov, Y. A. *Usp. Khim.* **1970**, *39*, 1560.
(52) Akhrem, A. A.; Ustynynk, T. K.; Titov, Y. A. *Russ. Chem. Rev.* **1970**, *39*, 732.
(53) March, J. *Advanced Organic Chemistry*; Wiley: New York, 1992; p 1080.
(54) le Noble, W. J. *Highlights of Organic Chemistry*; M. Dekker: New York, 1974; p 864.
(55) Chenier, P. J. *J. Chem. Educ.* **1978**, *55*, 286.
(56) Barbee, T. R.; Guy, H.; Heeg, M. J.; Albizati, K. F. *J. Org. Chem.* **1991**, *56*, 6773.
(57) Satoh, T.; Oguro, K.; Shishikura, J. *Tetrahedron Lett.* **1992**, *33*, 1455.
(58) Kimpe, N.; D_Hondt, L.; L., M. *Tetrahedron* **1992**, *48*, 3183.
(59) Satoh, T.; Oguro, K.; Shishikura, J. *Bull. Chem. Soc. Jpn.* **1993**, *66*, 2339.
(60) Satoh, T.; Motohashi, S.; Kimura, S. *Tetrahedron Lett.* **1993**, *34*, 4823.
(61) Lu, T.-J.; Liu, S.-W.; Wang, S.-H. *J. Org. Chem.* **1993**, *58*, 7945.
(62) Llera, J. M.; Fraser-Reid, B. *J. Org. Chem.* **1989**, *54*, 5544.
(63) Brik, M. E. *Synth. Commun.* **1990**, *20*, 1487.
(64) Lee, E.; Yoon, C. H. *J. Chem. Soc., Chem. Commun.* **1994**, *4*, 479.
(65) Sosnovsky, G.; Cai, Z.-W. *J. Org. Chem.* **1995**, *60*, 3414.
(66) Favorskii, A. E. *J. Prakt. Chem.* **1913**, *88*, 641.
(67) Aston, E. A. *J. Am. Chem. Soc.* **1940**, *62*, 2590.
(68) Richard *Compt. Rend.* **1933**, *197*, 1943.
(69) Richard *Compt. Rend.* **1935**, *200*, 1944.
(70) Tchoubar, B.; Sackur, O. *Compt. Rend.* **1939**, *208*, 1020.
(71) McPhee; Klingsberg *J. Am. Chem. Soc.* **1944**, *66*, 1132.
(72) Loftfield, R. B. *J. Am. Chem. Soc.* **1950**, *72*, 632.
(73) Loftfield, R. B. *J. Am. Chem. Soc.* **1951**, *73*, 4707.
(74) Andrés, J.; Bohm, S.; Moliner, V.; Silla, E.; Tuñón, I. *J. Phys. Chem.* **1994**, *98*, 6955.
(75) Tuñón, I.; Silla, E.; Bertrán, J. *J. Chem. Soc., Faraday Trans.* **1994**, *90*, 1757.
(76) Domingo, L. R.; Picher, M. T.; Andrés, J.; Moliner, V.; Safont, V. S. *Tetrahedron* **1996**, *52*, 10693.
(77) Castillo, R.; Moliner, V.; Safont, V. S.; Oliva, M.; Andrés, J. *J. Mol. Struct. (THEOCHEM)* **1998**, *426*, 299.
(78) Rivail, J. L.; Rinardi, D. *Chem. Phys*. **1976**, *18*, 233.
(79) Rinaldi, R.; Papalardo, R. R. SCRFPAC; Quantum Chemistry Program Exchange; Indiana University: Bloomington, IN, 1992; Program 622.
(80) Frisch, M. J.; Trucks, G. W.; Head-Gordon, M.; Gill, P. M.; Wong, M. W.; Foresman, J. B.; Johnson, B. G.; Schlegel, H. B.; Robb, M. A.; Replogle, E. S.; Gomperts, R.; Andres, J. L.; Raghavachari, K.; Binkley, J. S.; Gonzalez, C.; Martin, R. L.; Fox, D. J.; Defrees, D. J.; Baker, J.; Stewart, J. J. P.; Pople, J.A GAUSSIAN92, Revision G1; Gaussian Inc.: Pittsburgh, PA, 1992.
(81) Klamt, A.; Schüürmann, G. *J. Chem. Phys.* **1993**, *2*, 799.
(82) Stewart, J. J. P. *Acc. Chem. Res.* **1993**, *26*, 396.
(83) Jorgensen, W. L.; Chandrasekhar, J.; Madura, J. D.; Impey, R. W.; Klein, M. L. *J. Chem. Phys.* **1983**, *79*, 926.
(84) Brooks, C. L.; Karplus, M. *J. Mol. Biol.* **1989**, *208*, 159.
(85) Brooks, B. R.; Bruccoleri, R. E.; Olafson, B. D.; States, D. J.; Swaminathan, S.; Karplus, M. *J. Comput. Chem.* **1983**, *4*, 187.
(86) Turner, A. J. Doctoral Thesis, University of Bath, U.K., 1997.
(87) (a) Lee, C.; Yang, W.; Parr, R. G.; *Phys. Rev. B* **1988**, *37*, 785−789. (b) Becke, A. D. *Phys. Rev. A* **1988**, *38*, 3098−3100.